

Asteroseismology of Eclipsing Binary Stars in the *Kepler* Era

Daniel Huber^{1,2}

Abstract Eclipsing binary stars have long served as benchmark systems to measure fundamental stellar properties. In the past few decades, asteroseismology - the study of stellar pulsations - has emerged as a new powerful tool to study the structure and evolution of stars across the HR diagram. Pulsating stars in eclipsing binary systems are particularly valuable since fundamental properties (such as radii and masses) can be determined using two independent techniques. Furthermore, independently measured properties from binary orbits can be used to improve asteroseismic modeling for pulsating stars in which mode identifications are not straightforward. This contribution provides a review of asteroseismic detections in eclipsing binary stars, with a focus on space-based missions such as CoRoT and *Kepler*, and empirical tests of asteroseismic scaling relations for stochastic (“solar-like”) oscillations.

1 Introduction

Asteroseismology has undergone a revolution in the past few decades. Driven by multi-site ground-based observing campaigns and high-precision space-based photometry, the number of stars with detected pulsations has increased dramatically, and pulsation frequencies and amplitudes are measured with unprecedented precision. In particular the photometric data provided by the CoRoT and *Kepler* space telescopes have allowed the application of asteroseismology to stars throughout the HR diagram (e.g., Gilliland et al., 2010; Michel and Baglin, 2012; Chaplin and Miglio, 2013).

Owing to the relatively large apertures of some space-based telescopes, however, the majority of stars with high quality asteroseismic detections are relatively faint, and hence lack independent observational constraints from classical methods such

¹NASA Ames Research Center, Moffett Field, CA 94035, USA; e-mail: daniel.huber@nasa.gov

²SETI Institute, 189 Bernardo Avenue, Mountain View, CA 94043, USA

as astrometry or long-baseline interferometry. Combining independent observations with asteroseismology is crucial to advance progress in theoretical modeling of observed oscillation frequencies, and the validation of asteroseismic relations to derive fundamental stellar properties. Therefore, the full potential of asteroseismology can only be realized if such observations can be combined with model-independent constraints on properties such as temperatures, radii and masses.

Eclipsing binaries have long served as benchmark systems for determine fundamental properties of stars from first principles. Similar to measuring oscillation frequencies, the observation of photometric eclipses and spectroscopic radial velocities can be performed for relatively faint systems, as long as spectral lines of the components can be successfully disentangled. Furthermore, eclipses and pulsations can be measured using the same data. Thus, asteroseismology of components in eclipsing binary systems promises to be a powerful method to improve our understanding of stellar structure and evolution.

2 Principles of Asteroseismology

This chapter provides a brief introduction into the basic principles of asteroseismology. For a more thorough discussion the reader is referred to Christensen-Dalsgaard (2003), Aerts et al. (2010), and Handler (2013).

2.1 Types of Pulsation Modes

Single pulsation modes in spherically symmetric objects (i.e. in the absence of rapid rotation) can be described by the quantum numbers l , m and n . The spherical degree l corresponds to the total number of node lines on the surface, and the azimuthal order $|m|$ denotes the number of node lines that cross the equator. The azimuthal order takes values ranging from $-l$ to l (so that $2l + 1$ modes for each degree l), and is important for rotating stars for which the degeneracy imposed by spherical symmetry is broken. The special case of radial pulsations is expressed as $l = 0$, and corresponds to the star expanding and contracting as a whole (sometimes also called the “breathing mode”). Spherical degrees greater than zero are non-radial pulsations, with $l = 1$ being dipole, $l = 2$ quadrupole and $l = 3$ octupole modes. Figure 1 shows examples of pulsations modes for several configurations of l and m . Note that since stars are observed as point sources, cancellation effects generally prevent the observation of high degree ($l > 3$) modes. In addition to l and m , oscillation modes are further characterized by the radial order n , the number of nodes along a radius from the surface to the center of the star.

Stellar pulsations can furthermore be separated into two main types: pressure modes (p modes) and gravity modes (g modes). Pressure modes are acoustic waves propagating through the stellar interior by the compression and decompression of

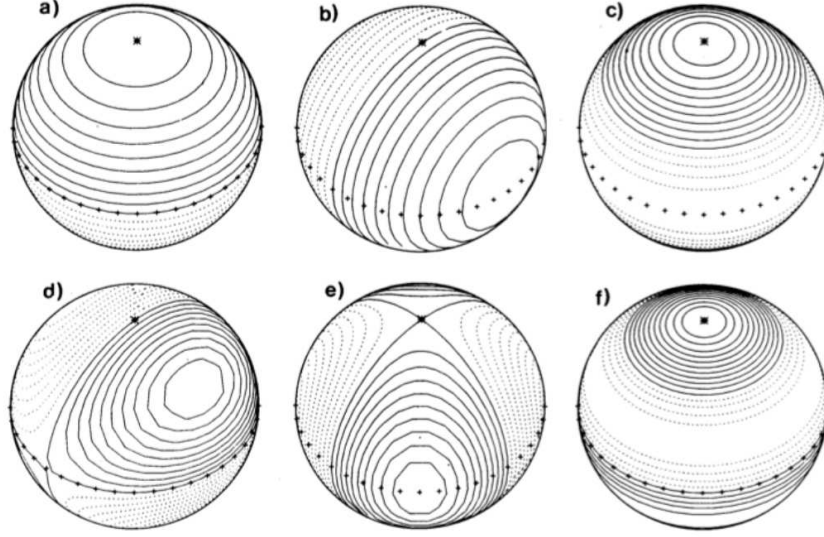


Fig. 1 Examples of spherical harmonics used to describe stellar pulsation modes. Solid lines show parts of the star moving towards the observer, dotted lines parts that move away. The pole of the star is indicated by star-signs, the equator by plus-signs. The following cases are shown: a) $l = 1$, $m = 0$; b) $l = 1$, $m = 1$; c) $l = 2$, $m = 0$; d) $l = 2$, $m = 1$; e) $l = 2$, $m = 2$; f) $l = 3$, $m = 0$. From Christensen-Dalsgaard (2003).

gas, and the pressure gradient acts as the restoring force. Gravity modes correspond to pulsations due to the interplay of buoyancy and gravity, and buoyancy acts the restoring force. Note that for g modes, no radial ($l = 0$) modes exist and the radial order n is conventionally counted negative. The propagation zones of p modes and g modes are generally determined by the position of convection zones. Gravity modes are heavily damped in zones where convection is unstable, and hence are usually confined to the deep interior for cool stars. Pressure modes, on the other hand, propagate in radiative zones, and hence are more easily excited to observational amplitudes on the surface. For evolved stars, the p-mode and g-mode cavity can overlap, giving rise to so-called “mixed modes” (Dziembowski et al., 2001). Such modes are of particular importance for studying interior properties since they contain contribution from g modes confined to the core, but can be observed near the surface. For massive stars with large convective cores g modes are more typically observed.

2.2 Excitation Mechanisms

Stellar pulsations are excited across a wide range of temperatures and evolutionary states in the H-R diagram (see Figure 2). The excitation mechanism driving these oscillations can be broadly divided into two main types.

2.2.1 Stochastic Oscillations

Oscillations in cool, low-mass stars like our Sun are excited by turbulent convection in the outer layers of the star (see, e.g., Houdek et al., 1999). The acoustic energy in the convection zone damps and excites oscillation modes stochastically, resulting in mode lifetimes as short as a few days in stars similar to our Sun. Finite mode lifetimes cause the peaks in the oscillation spectrum to be broadened into a Lorentzian shape, and hence such oscillations typically contain no phase information. Stochastic oscillations are commonly referred to as solar-like oscillations, although they are also found in more evolved stars with convective envelopes such as red giants.

Stochastic oscillations are typically of high radial order n . Oscillation frequencies $\nu_{n,l}$ of high radial order n and low spherical degree l can be described by the asymptotic theory of stellar oscillations (Vandakurov, 1968; Tassoul, 1980; Gough, 1986), which observationally can be approximated as follows:

$$\nu_{n,l} \approx \Delta \nu \left(n + \frac{1}{2}l + \varepsilon \right) - \delta \nu_{0l}. \quad (1)$$

Equation (1) predicts that oscillation frequencies follow a series of characteristic spacings. The large frequency separation $\Delta \nu$ is the separation of modes of the same spherical degree l and consecutive radial order n , while modes of the different degree l and same radial order n are expected to be separated by the small frequency separations $\delta \nu_{0l}$. The constant ε in Equation (1) is related to the inner and outer turning point of the oscillations, and therefore depends on the properties of the surface layers of the star.

In the asymptotic theory, the large frequency separation can be shown to be the inverse of twice the sound travel time from the surface to the center (Ulrich, 1986; Christensen-Dalsgaard, 2003):

$$\Delta \nu = \left(2 \int_0^R \frac{dr}{c} \right)^{-1}, \quad (2)$$

where the sound speed c , assuming adiabaticity, is given by

$$c = \sqrt{\Gamma_1 p / \rho}. \quad (3)$$

Here, Γ_1 is an adiabatic exponent, p is the pressure and ρ is the density. For an ideal gas $\rho \propto \mu P / T$, and therefore

$$c \propto \sqrt{T / \mu}. \quad (4)$$

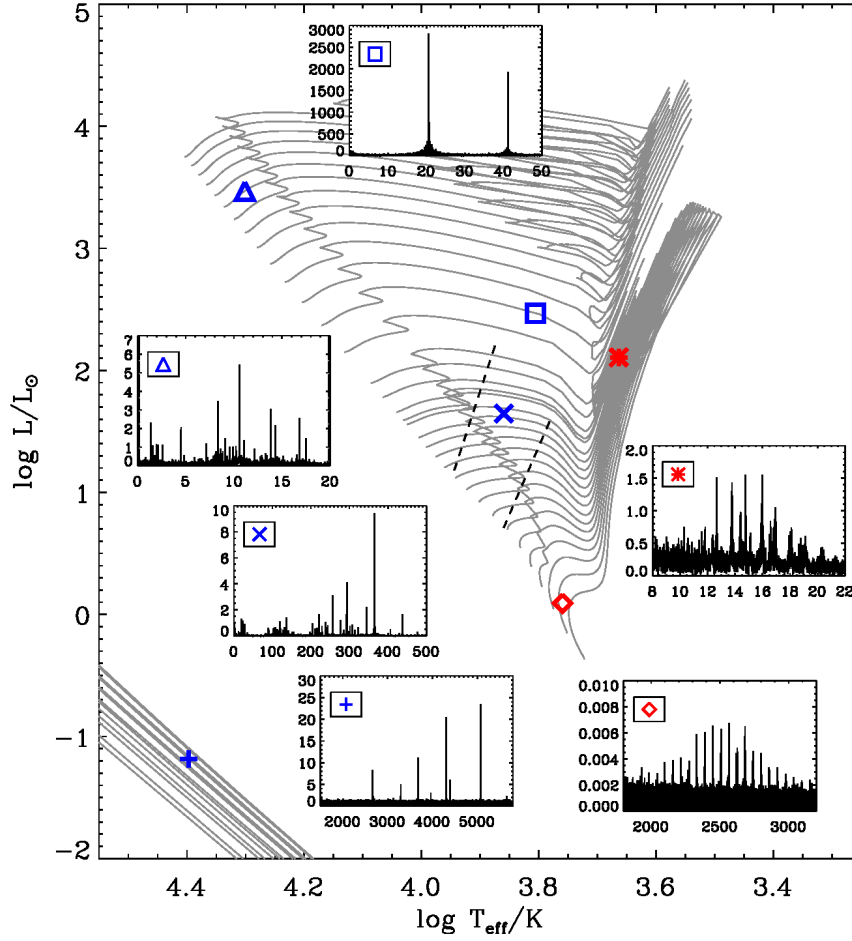


Fig. 2 H-R diagram illustrating different types of pulsating stars. Grey lines are BaSTI evolutionary tracks (Pietrinferni et al., 2004) and white-dwarf cooling curves (Salaris et al., 2010). Insets show amplitude spectra in units of ppt versus μHz for six typical stars based on *Kepler* data: the Sun-like oscillator 16 Cyg B (red diamond, Metcalfe et al., 2012), the red giant KIC 5707854 (red asterisk), the hybrid γ Dor- δ Scuti pulsator KIC 11445913 (blue cross, Grigahcène et al., 2010), the hybrid SPB- β Cep pulsator KIC 3240411 (blue triangle, Lehmann et al., 2011), the RR Lyrae star V354 Lyr (blue square, Nemec et al., 2013) and the white dwarf KIC 8626021 (blue plus symbol, Østensen et al., 2011). Red and blue symbols denote stars with stochastic and coherent oscillations, respectively. Dashed lines show the blue and red edge of the δ Scuti instability strip (Pamyatnykh, 2000).

The sound speed depends on the average internal temperature and chemical composition of the gas. For an ideal gas, basic estimates for the central temperature give $T \propto \mu M/R$ (Kippenhahn and Weigert, 1994), and hence

$$\Delta \nu \propto \left(\frac{M}{R^3} \right)^{1/2}. \quad (5)$$

The large frequency separation is therefore a direct measure of the mean stellar density.

Figure 2 shows that the power excess of stochastic oscillations has a roughly Gaussian shape, reaching a maximum at a certain frequency. This maximum defines the frequency of maximum power (ν_{\max}) as well as the maximum amplitude of the oscillation, which are related to the driving and damping of the modes. The frequency of maximum power has been suggested to scale with the acoustic cut-off frequency (Brown et al., 1991), which is the maximum frequency below which an acoustic mode can be reflected (Christensen-Dalsgaard, 2003):

$$\nu_{\text{ac}} = \frac{c}{2H_p}. \quad (6)$$

Here, H_p is the pressure scale height which, for an isothermal atmosphere, is given by (Kippenhahn and Weigert, 1994):

$$H_p = \frac{PR^2}{GM\rho}. \quad (7)$$

Using the same approximation as above for an ideal gas and assuming that the temperature can be approximated by the effective temperature T_{eff} , we have:

$$\nu_{\max} \propto \nu_{\text{ac}} \propto \frac{M}{R^2 \sqrt{T_{\text{eff}}}}. \quad (8)$$

Actual frequency spectra are considerably more complex than described in the above paragraphs. For example, frequency separations show variations as a function of radial order which depend on the sound speed profile, and hence can be used to infer details on the interior structure such as the depth of convection zones or stellar ages (e.g., Aerts et al., 2010). However, the simple Equations (5) and (8) readily relate observables to mass and radius, and therefore in principle offer a straightforward way to calculate these properties. Importantly, these relations are only approximate and require careful calibration over a range of evolutionary states. One of the important prospects of asteroseismology in eclipsing binary stars is to accurately calibrate these scaling relations.

2.2.2 Coherent Pulsations

In hotter stars ($T_{\text{eff}} \gtrsim 6500\text{K}$) pulsations can be driven by temperature-dependent opacity changes causing radiation pressure to continuously expand a star past its

equilibrium before contracting again under the force of gravity. This heat-engine mechanism (also called κ mechanism) acting in the hydrogen and helium ionization zones is effective in a region of the H-R diagram referred to as the classical instability strip, which includes pulsators such as δ Scuti stars, RR-Lyrae stars, and Cepheids (see Figure 2). Pulsations driven by the κ mechanism acting in iron-group elements drive pulsations in stars hotter than the classical instability strip, such as slowly pulsating B stars and beta Cephei variables. Coherent (also called “classical”) pulsations are phase-stable over long timespans of stellar evolution, and typically show significantly higher amplitudes than stochastic oscillations (Figure 2).

Coherent pulsations can also be driven by a heat-engine mechanism which operates at the base of the outer convection zone (“convective blocking”, Guzik et al., 2000). This mechanism is the favored explanation for g modes observed in γ Dor stars, which border stochastically-driven oscillators and δ Scuti pulsators in the H-R diagram, as well as H-atmosphere white dwarfs (DAV or ZZ Ceti stars). Theoretically the κ mechanism, convective blocking and stochastic driving should be able to excite oscillations simultaneously for stars near the red edge of the instability strip. Recent space-based observations have established that hybrid γ Dor- δ Scuti pulsators are indeed common (Grigahcène et al., 2010), and first evidence for hybrid coherent-stochastic pulsators have been found (Antoci et al., 2011).

3 The Importance of Eclipsing Binary Stars for Asteroseismology

3.1 Asteroseismic Scaling Relations

Observables of stochastic oscillations can be trivially related to fundamental stellar properties by scaling from the observed values of the Sun. For example, Equations (5) and (8) can be rearranged to solve for stellar mass and radius:

$$\frac{M}{M_{\odot}} = \left(\frac{v_{\max}}{v_{\max, \odot}} \right)^3 \left(\frac{\Delta \nu}{\Delta \nu_{\odot}} \right)^{-4} \left(\frac{T_{\text{eff}}}{T_{\text{eff}, \odot}} \right)^{3/2}, \quad (9)$$

$$\frac{R}{R_{\odot}} = \left(\frac{v_{\max}}{v_{\max, \odot}} \right) \left(\frac{\Delta \nu}{\Delta \nu_{\odot}} \right)^{-2} \left(\frac{T_{\text{eff}}}{T_{\text{eff}, \odot}} \right)^{1/2}. \quad (10)$$

The large frequency separation $\Delta \nu$ and the frequency of maximum power ν_{\max} can be easily measured from the power spectrum, providing a straightforward (and in principle model-independent) method to determine fundamental properties of stars. While matching individual oscillation frequencies to stellar models typically yields more precise and detailed information (e.g. on initial helium abundances and ages), scaling relations have two important applications. First, due to the low amplitudes of stochastic oscillations, the signal-to-noise is frequently too low to reliably extract a significant number of oscillation modes, and only the average large separation can

be determined. Second, the measurement of Δv and v_{\max} can be performed automatically, and hence enables the application of asteroseismology to a large number of stars simultaneously. This new era of “ensemble asteroseismology” has been recently made possible with the launch of space telescopes such as CoRoT and *Kepler*, which provide high-precision photometry for thousands of stars.

To illustrate this, Figure 3 summarizes the detections of stochastic oscillations over the past ~ 20 years. Starting with the first confirmed detection of oscillations in Procyon by Brown et al. (1991), subsequent ground-based radial-velocity campaigns (e.g., Bouchy and Carrier, 2001; Carrier et al., 2001; Kjeldsen et al., 2005; Bedding et al., 2010) as well as observations with early space telescopes such as MOST (Matthews, 2007; Guenther et al., 2007) yielded detections in about a dozen bright stars. Launched in 2006, the CoRoT space telescope delivered the first high signal-to-noise detections in main-sequence stars (Michel et al., 2009), and led to the breakthrough discovery of non-radial modes in thousands of red giants (De Ridder et al., 2009; Hekker et al., 2009; Mosser et al., 2010). The *Kepler* space telescope, launched in 2009, continued the revolution of cool star asteroseismology by filling up the low-mass H-R diagram with detections, including dwarfs cooler than the Sun (Chaplin et al., 2011b) and over ten thousand red giants (Stello et al., 2013). The larger number of red giants with detected oscillations is due to a combination of two effects: First, oscillation amplitudes increase with luminosity (Kjeldsen and Bedding, 1995), making a detection easier at a given apparent magnitude. Second, the majority of stars observed by *Kepler* are observed with 30-minute sampling, setting a limit of $\log g \lesssim 3.5$ since less evolved oscillate above the Nyquist frequency.

It is in particular the large number of oscillating giants which drive the need to validate scaling relations. By combining asteroseismic radii and masses with temperatures and metallicities, stellar ages can be determined for thousands of giant stars, opening the door to galactic stellar population studies. Indeed, follow-up surveys using multi-object spectrographs such as APOGEE (Mészáros et al., 2013) or Stromgren photometry (Casagrande et al., 2014) have been already dedicated for this purpose. The success of this new era of galactic archeology relies on our ability to empirically calibrate asteroseismic scaling relations.

Testing the accuracy of scaling relations is an active field of research (see Belkacem, 2012; Miglio et al., 2013, for reviews). Theoretical work has shown that both relations typically hold to a few percent (Stello et al., 2009; Belkacem et al., 2011), although deviations of the Δv scaling relation by up to 2% have been reported for dwarfs with $M/M_{\odot} > 1.2$ (White et al., 2011). Revised scaling relations based on model frequencies (White et al., 2011) and extrapolating the measurement of Δv to higher radial orders (Mosser et al., 2013) have been proposed, although some doubt about the applicability of the latter revision has been expressed (Hekker et al., 2013). Empirical tests have relied on independently measured properties from Hipparcos parallaxes, clusters, and long-baseline interferometry (see, e.g., Stello et al., 2008; Bedding, 2011; Brogaard et al., 2012; Miglio, 2012; Miglio et al., 2012; Huber et al., 2012; Silva Aguirre et al., 2012). For unevolved stars ($\log g \gtrsim 3.8$) no empirical evidence for systematic deviations has yet been de-

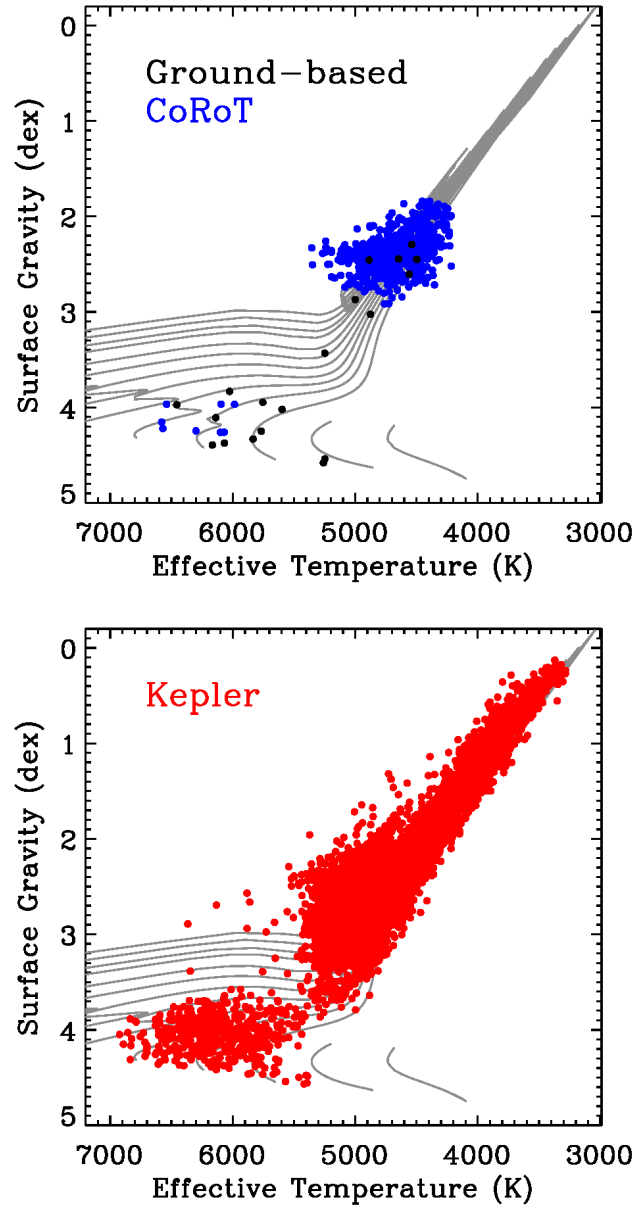


Fig. 3 Surface gravity versus effective temperature for stars with detected stochastic oscillations as of early 2014. Colors illustrate detections by ground-based campaigns (black, top figure), CoRoT (blue, top figure) and *Kepler* (red, bottom figure). Grey lines are solar-metallicity evolutionary tracks to guide the eye. CoRoT red giant detections and *Kepler* detections are taken from the catalogs by Hekker et al. (2009) and Huber et al. (2014), respectively.

terminated within the observational uncertainties, but for giants a systematic deviation of $\sim 3\%$ in $\Delta\nu$ has been noted for He-core burning red giants (Miglio et al., 2012).

A common limitation is that a separate test of the $\Delta\nu$ and ν_{\max} scaling relation relies on an *independent* knowledge of stellar mass and radius. Such information is typically only available in binary systems, either if the masses and radii are measured through an astrometric orbit and interferometry, or in doubled-lined spectroscopic eclipsing binaries for which absolute masses and radii can be measured. So far, such a test has only been possible for three stars: α Cen A, α Cen B, and Procyon A.

3.2 Mode Identification and Driving Mechanisms in Intermediate Mass Stars

Asteroseismology of classical pulsators has been successfully performed for several decades using ground-based photometric and spectroscopic campaigns (e.g., Breger, 2000). Intermediate and high mass stars probe parameter space which are plagued by model uncertainties such as convective core-overshooting and the effects of rotation (e.g., Aerts, 2013). Hence, asteroseismology holds great promise to improve our understanding of the evolution of such stars. A serious problem, however, is that classical pulsators often show complex frequency spectra which do not allow mode identification based on simple pattern recognition. In such cases mode identifications rely on measuring amplitudes in multicolor photometry or spectroscopic line-profile variations, although more recent observations have revealed evidence for systematic structure in the frequency spectra of δ Scuti stars (Breger et al., 2011)¹.

Classical pulsators in eclipsing binary stars offer the possibility to alleviate this problem. Creevey et al. (2011) found that eclipsing binaries constrain fundamental properties of a star equally well or better than what is possible for a pulsating δ Scuti star with correct mode identification (Figure 4). Conversely, the correct mode identification can be inferred by comparing solutions assuming different mode identifications, and identifying those solutions which yield the best match to the binary constraints. Once the mode identification is secured, interior properties (such as convective core overshoot or mixing length parameter) can be further constrained using the pulsation frequencies.

Eclipsing binary systems may also contribute to addressing the long-standing question of driving mechanisms near the red edge of the instability strip. Stochastic oscillations in δ Scuti and γ Dor stars have been predicted theoretically, yet little conclusive observational evidence for hybrid oscillators has yet been found. Pulsating stars with precisely determined fundamental properties may be key to understand the interplay between convection and driving of pulsations near the red edge of the classical instability strip.

¹ An important exception are rapidly oscillating Ap stars, a class of coherent pulsators showing regularly-spaced high-order p modes (Kurtz, 1982).

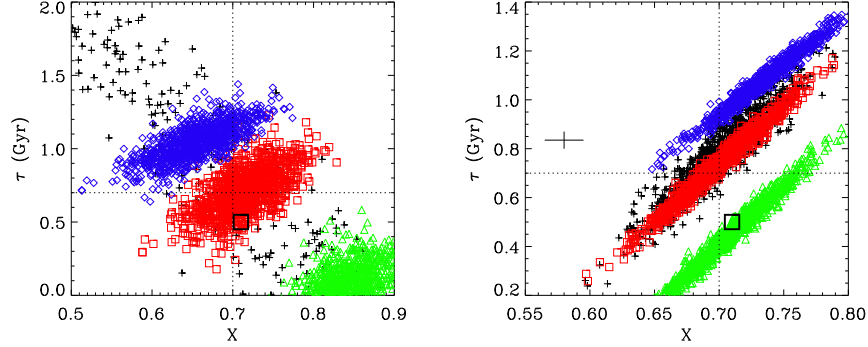


Fig. 4 Fitted age versus initial hydrogen abundance for simulated data of a single pulsating δ Scuti star (left panel) and an eclipsing binary including a δ Scuti star (right panel). Symbols denote simulations including no pulsation mode (black plus signs), including a pulsation frequency with a correct mode identification (red squares), including a pulsation frequency with incorrect spherical degree (blue diamonds), and a pulsation frequency with incorrect radial order (green triangles). Dashed lines mark the exact input solution, the box show the initial guess values, and the error bar mark the input uncertainties for the eclipsing binary solution. From Creevey et al. (2011).

3.3 Tidally Induced Pulsations and Eccentric Binary Systems

Multiple star systems offer the possibility to study gravity modes driven by tidal interactions (dynamical tides, Zahn, 1975), which are particularly prominent in eccentric binary systems (e.g., Lai, 1997). Tidal interactions can also be used to infer properties such as eccentricities, masses and inclinations of binary stars and are of importance for planet formation, for example for migration theories of hot Jupiters through high eccentricity migration and tidal circularization (e.g., Winn et al., 2010).

Observations of dynamical tides have long been hampered by the required high precision photometry and continuous coverage to observe these effects over many orbital periods. *Kepler* changed this picture by observationally confirming a new class of eccentric binaries with tidally induced brightness variations at periastron passage, also known as “heartbeat” stars (Thompson et al., 2012). The prototype, KOI-54, consists of two nearly equal mass A stars in a highly eccentric orbit (Welsh et al., 2011) with tidally induced pulsations that may be locked into resonance with the binary orbit (Fuller and Lai, 2012; Burkart et al., 2012). The discovery of KOI-54 started a new era of observational “tidal asteroseismology”.

While tidal interactions carry a large amount of information about binary systems, challenges remain which can be addressed if constraints from eclipses are available. For example, the precise frequencies, amplitudes, and phases of tidally excited oscillations may provide a wealth of information on tidal damping mechanisms. Independently measured radii and masses of the components provide a possibility to accurately model the stellar components and calibrate theories of tidal dissipation.

4 Giant Stars

Eclipsing binary systems provide several powerful possibilities to study the structure and evolution of giant stars, for example through the observation of chromospheric eclipses. Due to the large oscillation amplitudes and the presence of mixed modes, red giant stars also have large potential for asteroseismic studies.

4.1 Oscillating Giants in Eclipsing Binary Systems

The first detection of an oscillating giant in an eclipsing binary system was presented by Hekker et al. (2010) using *Kepler* data. Figure 5 shows the discovery light curve of KIC 8410637 (TYC 3130-2385-1, $V = 11.3$) based on the first 30 days of *Kepler* data, revealing a total eclipse (top panel) and stochastic oscillations (bottom panel). The presence of oscillations during the eclipse pointed to a smaller object being occulted by a red giant. Since only a single eclipse was observed, the orbital period of the system was initially unknown, but constraints through the luminosity and radius ratio suggested a F-type main-sequence star as the secondary component.

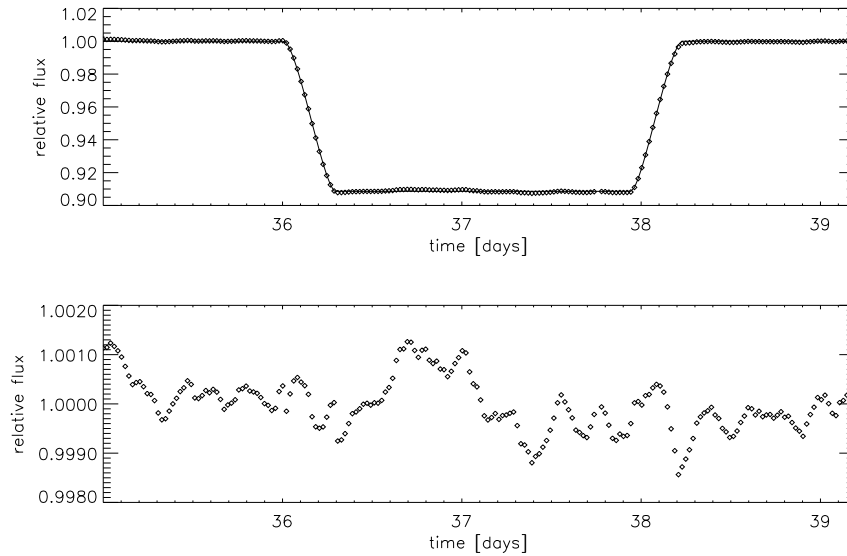


Fig. 5 Top panel: *Kepler* discovery light curve of KIC 8410637, the first eclipsing binary with an oscillating red giant component. Bottom panel: Light curve after correcting an eclipse model, revealing the oscillations in the red giant primary. From Hekker et al. (2010).

Frandsen et al. (2013) presented a complete orbital solution of KIC 8410637 based on nearly 1000 days of *Kepler* data, an extensive radial-velocity campaign and multi-color ground-based photometry. Figure 6 shows the radial-velocity solution, which combined with the extended *Kepler* dataset spanning three primary and three secondary eclipses was used to derive a dynamical solution of the system, with an orbital period of 408 days and an eccentricity of 0.6. The radius and mass of the components were measured to be $R_{\text{RG}} = 10.74 \pm 0.11 R_{\odot}$ and $M_{\text{RG}} = 1.56 \pm 0.03 R_{\odot}$ for the red-giant primary, as well as $R_{\text{MS}} = 10.74 \pm 0.11 R_{\odot}$ and $M_{\text{MS}} = 1.56 \pm 0.03 R_{\odot}$ for main-sequence secondary. The exquisite precision of the absolute radii and masses make KIC 8410637 an extremely interesting object to test asteroseismic scaling relations for evolved stars.

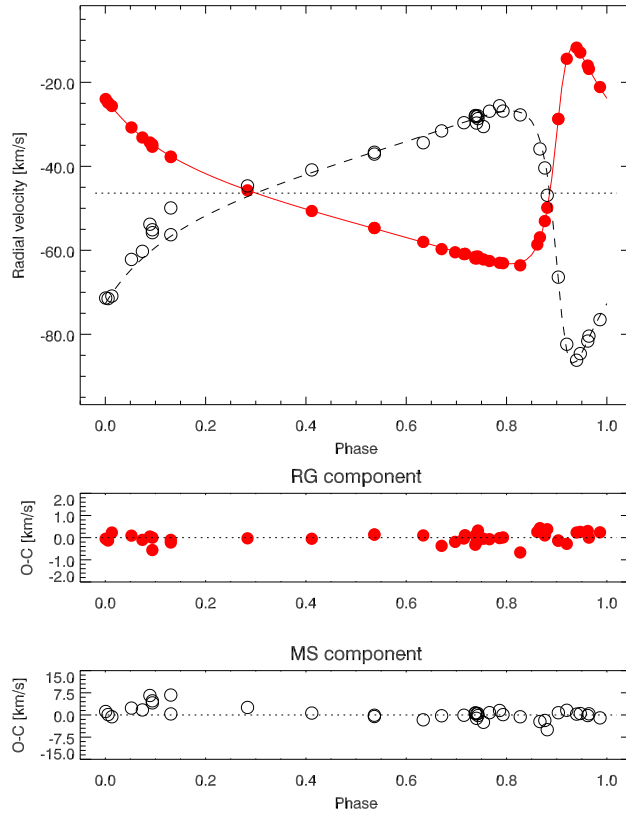


Fig. 6 Top panel: Radial velocities phased with the 408 day orbital period of the red giant primary (red filled circles) and main-sequence secondary (black open circles) component of KIC 8410637. Bottom panels: Residuals of the best-fitting model solution. KIC 8410637 is the first eclipsing binary with a component showing stochastic oscillations and a measured double-lined spectroscopic orbit. From Frandsen et al. (2013).

Table 1 compares the solution by Frandsen et al. (2013) to the values from scaling relations presented by Hekker et al. (2010). While the values are in reasonable agreement, the uncertainties on the seismic mass and radius are fairly large since the analysis by Hekker et al. (2010) was based on only 30 days of *Kepler* data. To test whether this difference is significant, the analysis was repeated using data from Q0-16 (1350 days) with the method by Huber et al. (2009). The resulting seismic values are $v_{\max} = 46.2 \pm 1.1 \mu\text{Hz}$ and $\Delta v = 4.634 \pm 0.012 \mu\text{Hz}$, in good agreement with the values by Hekker et al. (2010) but with significantly reduced uncertainties (factor of 2 in mass and radius). Combining these values with the effective temperature by Frandsen et al. (2013) yields excellent agreement (within 0.003 dex) in $\log g$ (see Table 1). However, the density is underestimated by $\sim 7\%$ (1.8σ , taking the uncertainty in the seismic and dynamical density into account), which results in an overestimate of the radius by $\sim 9\%$ (2.7σ) and mass by $\sim 17\%$ (1.9σ). Note that a $\sim 7\%$ difference in density is a factor 7 larger than the typical formal uncertainty on the seismic density from the measurement of Δv using different methods (Hekker et al., 2012). Table 1 also lists radius and mass estimates using the recently proposed corrections to the Δv scaling relation by White et al. (2011) and Mosser et al. (2010). Both corrections reduce the differences to $\sim 4\%$ in density, $\sim 5\%$ in radius, and $\sim 10\%$ in mass.

An important piece of information for KIC 8410637 is whether the primary is a He-core burning red clump star or still ascending the red-giant branch. While an asteroseismic determination of the evolutionary state based on gravity-mode period spacings (Bedding et al., 2011; Beck et al., 2011) is still pending, Frandsen et al. (2013) argued that a red-clump phase of the primary is more likely based on the comparison of the derived temperature with isochrones. However, relative corrections to the Δv scaling relation between red-clump and RGB stars tend to increase the seismic mass and radius (Miglio et al., 2012), hence resulting in even larger differences with the orbital solution. Additionally, as pointed out by Frandsen et al. (2013), the small periastron distance would imply that the system may have undergone significant mass transfer when the primary reached the tip of the RGB.

Table 1 Fundamental properties of the red giant component in the eclipsing binary system KIC 8410637 from an orbital solution and from asteroseismic scaling relations.

Parameter	RVs+EB	Asteroseismic Scaling Relations			
	Frandsen et al.	Hekker et al.	Q1-16*	Q1-16+White [‡]	Q1-16+Mosser [‡]
T_{eff} (K)	4800 ± 80	4650 ± 80	4800 ± 80	4800 ± 80	4800 ± 80
R (R_{\odot})	10.74 ± 0.11	11.8 ± 0.6	11.58 ± 0.30	11.23 ± 0.29	11.31 ± 0.29
M (M_{\odot})	1.56 ± 0.03	1.7 ± 0.3	1.83 ± 0.14	1.72 ± 0.13	1.74 ± 0.13
$\log g$ (cgs)	2.569 ± 0.009	—	2.572 ± 0.011	2.572 ± 0.011	2.572 ± 0.011
ρ ($\rho_{\odot} \times 10^3$)	$1.259 \pm 0.046^{\dagger}$	—	1.1765 ± 0.0061	1.2132 ± 0.0063	$1.2047 \pm 0.0061^{\dagger}$

* For asteroseismic solutions based on Q1-Q16, solar reference values of $v_{\max, \odot} = 3090 \pm 30 \mu\text{Hz}$ and $\Delta v_{\odot} = 135.1 \pm 0.1 \mu\text{Hz}$ were used (Huber et al., 2011).

[‡] Based on scaling relations corrections proposed by White et al. (2011) and Mosser et al. (2013).

[†] Calculated from mass and radius.

Clearly, larger samples are required to determine whether the differences found for KIC 8410637 may be systematic. Fortunately, the *Kepler* offers a goldmine of over 15,000 oscillating giant stars which have been used to identify additional systems. Gaulme et al. (2013) crossmatched the *Kepler* eclipsing binary catalog (Prša et al., 2011; Slawson et al., 2011; Matijević et al., 2012) with red giants classified in the Kepler Input Catalog (Brown et al., 2011) to identify 12 new candidate eclipsing binary systems with oscillating red giants. The red giant components in the sample span a large range in evolution, making this sample promising to extend tests of asteroseismic scaling relations. Radial velocity follow-up to confirm these systems as genuine eclipsing binaries with oscillating giants and to measure absolute radii and masses are currently underway.

4.2 Oscillating Giants in Eccentric Binary Systems

The first oscillating giants in heartbeat systems were presented by Beck et al. (2013), who confirmed the discovery of 18 Kepler systems through radial-velocity follow-up. Figure 7 shows five examples of phased heartbeat light curves. The shape, length and amplitude of the light distortion depends on the orientation and inclination of the orbit, as well as the masses of the components.

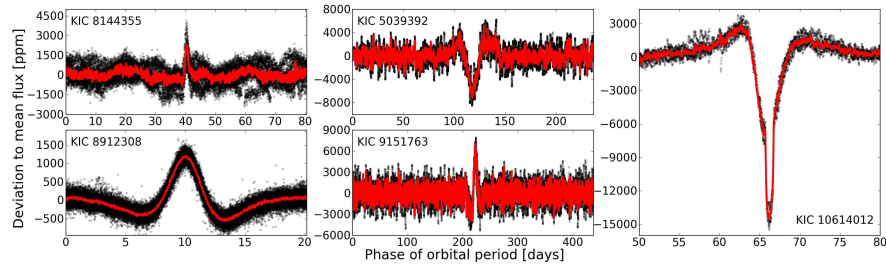


Fig. 7 *Kepler* phase curves of five eccentric binary systems with oscillating red giants displaying gravitationally induced brightness changes near periastron passage (“heartbeat” stars). The shape and amplitude of the distortion depends on the orbital properties (e.g. eccentricity, argument of periastron, inclination) and masses of the system. From Beck et al. (2013).

Beck et al. (2013) presented a detailed study of KIC5006817, a system with an orbital period of 95 days, eccentricity of 0.7, and an orbital inclination of 62 degrees. While the secondary is too faint to be detected in the spectra, the primary is relatively unevolved RGB star ($R = 5.84 R_{\odot}$, $M = 1.49 M_{\odot}$) showing a high signal-to-noise asteroseismic detection. The asteroseismic analysis allowed a measurement of the stellar inclination axis from rotationally split dipole modes (Gizon and Solanki, 2003) of 77 ± 9 degrees. The larger value compared to the orbital inclination and the

comparison of the rotation period inferred from rotational splittings to the orbital period were interpreted as evidence that the system has not yet tidally synchronized.

The analysis of KIC 5006817 yielded several surprising results. First, the data show an apparent absence of a signal due to Doppler beaming, a periodic increase and decrease in intensity mostly due to the radial velocity shift of the stellar spectrum relative to the photometric bandpass. Second, the gravity darkening derived from the light curve model disagrees with empirical and semi-empirical gravity darkening values. While the former may be related to the difficulty of detrending data when the orbital period is similar to the length of a Kepler observing quarter, Beck et al. (2013) conclude that the latter likely implies a revision of commonly accepted gravity darkening exponents for giants (assuming that the derived properties of the red giant are correct).

While the absence of eclipses and the spectroscopic non-detection of the secondary precluded an independent measurement of radii and masses of both components, heartbeat systems such as KIC 5006817 allow insights into the dynamical evolution of eccentric binary systems with evolved stars. For example, Beck et al. (2013) find tentative evidence that systems with higher larger red-giant primary radii have longer orbital periods, indicating that some of these systems may form the progenitors of cataclysmic variables or subdwarf B stars. Interestingly, the prototype eclipsing binary KIC 8410637 does not show heartbeat events, although its orbital properties are compatible with the sample by Beck et al. (2013).

4.3 Giants in Hierarchical Triple Systems: The Case of HD181068

An exciting discovery in the early phases of the *Kepler* mission was the existence of hierarchical triply eclipsing triple systems. The first example, presented by Carter et al. (2012), consists of three low-mass main-sequence stars and allowed a full dynamical solution of all components by measuring eclipse-timing variations, without the need for radial-velocity follow-up observations (a technique that was also applied to confirm numerous multi-planet systems, e.g. Fabrycky et al., 2012).

Shortly after, Derekas et al. (2011) presented the discovery of the first triply eclipsing triple system with a red-giant component. Figure 8 shows the discovery light curve of HD 181068 (also known as “Trinity”), which contains long-duration eclipses with an interval of ~ 23 days interleaved by short-duration eclipses with an interval of ~ 0.4 days. Follow-up radial velocity and interferometric observations confirmed that the primary is a red giant which is eclipsed by a pair of main-sequence stars with an orbital period of 45.5 days, while the low-mass binary itself eclipses every ~ 0.9 days. The short-period eclipses disappear during primary and secondary eclipse (see Figure 8) because of the similar temperatures (and hence surface brightnesses) of the three components. Subsequent modeling of eclipse timing variations of the outer binary yielded a full dynamical solution, with radii and masses of all three components measured to better than 5% (Borkovits et al., 2013).

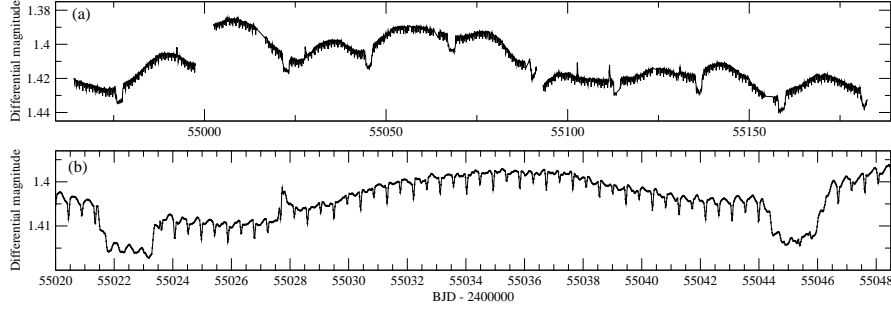


Fig. 8 Discovery light curve of HD 181068, a triply eclipsing triple system consisting of a red giant primary and two main-sequence stars. The bottom panel shows a close-up of one orbital period with a primary and secondary eclipse, interleaved by ~ 0.9 d eclipses of the main-sequence binary. From Derekas et al. (2011).

A remarkable aspect of the HD 181068 system is the lack of stochastic oscillations. Figure 9 compares a power spectrum of HD181068 (after removing all eclipses) to an oscillating field giant with similar fundamental properties as HD181068 A. Interestingly the granulation background, which manifests itself as red noise in the power spectrum, is very similar in both stars, while the power excess due to oscillations is completely suppressed in HD181068 A. As speculated by Fuller et al. (2013), the close dwarf components may be responsible for this suppression by tidally synchronizing the rotational frequency of the red giant with the long-period orbit, and causing increased magnetic activity which has been suggested to suppress the excitation of stochastic oscillations (Chaplin et al., 2011a). HD181068 A is the first confirmed case of suppressed stochastic oscillations in a binary system, and further evidence that this suppression mechanism is indeed related to the binary interactions has been recently found for other candidate eclipsing binaries with red-giant components (Gaulme et al., 2014).

While no stochastic oscillations are observed, HD 181068 A shows high amplitude pulsations at lower frequencies, which can be clearly identified during primary and secondary eclipse (Figure 8). The peaks in the amplitude spectrum are narrow, indicating that they are not stochastically driven, and are linear combinations of the long (ω_1) and short orbital frequency (ω_{23}) with frequencies of $f_1 = 2(\omega_{23} - 2\omega_1)$, $f_2 = 2(\omega_{23} - \omega_1)$, $f_3 = \omega_{23}$ and $f_4 = 2\omega_{23}$. Fuller et al. (2013) demonstrated that these frequencies can be explained by three body tidal forces, which cause the orbital motion of the outer pair to induce pulsations in red-giant primary.

5 Dwarf and Subgiant Stars

Asteroseismology of dwarfs and subgiants in eclipsing binaries has traditionally focused on coherent pulsators such as δ Scuti and γ Dor stars, since these show

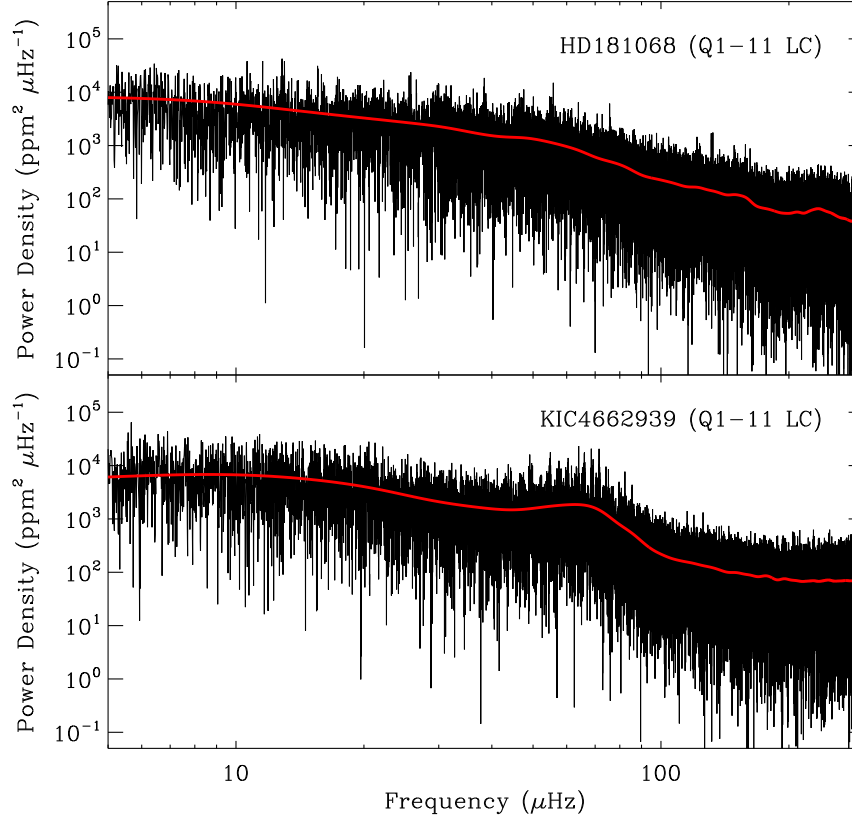


Fig. 9 Top panel: Power spectrum of HD 181068 after removal of the eclipses from the *Kepler* light curve. The thick red line shows a heavily smoothed version of the spectrum. Bottom panel: Power spectrum of KIC 4662939, a field red giant with similar fundamental properties as HD 181068 A. Note the absence of stochastic oscillations near 70 μHz in the top panel. From Fuller et al. (2013).

larger amplitudes than stochastic oscillators and hence eclipses and pulsations can be more easily detected using ground-based observations. At the time of writing of this review no stochastic oscillations in a dwarf or subgiant component in an eclipsing binary have been published, although at least two *Kepler* detections are in preparation (Basu et al. & Sharp et al., in preparation).

5.1 Classical Pulsators

Classical pulsations in A and F stars have been successfully detected using ground-based observations in a few dozen detached and semi-detached eclipsing binary sys-

tems (see, e.g., Mkrtychian et al., 2004; Rodríguez and Breger, 2001, and references therein). However, the short time base and precision of ground-based photometry often limited the number of reliable pulsation frequencies that were detected, and only for a small number of these systems full dynamical orbits could be combined with a secure detection of high-amplitude pulsations (see, e.g., Christiansen et al., 2007).

Similar to stochastic oscillations, CoRoT and *Kepler* dramatically changed this picture. Following first detections of γ Dor pulsations in eclipsing binaries discovered by CoRoT (Damiani et al., 2010; Sokolovsky et al., 2010), Maceroni et al. (2009) presented a radial velocity orbit of an eclipsing binary consisting of two B stars, with additional variations that could either be attributed to self-driven or tidally induced pulsations. Firm detections of self-excited γ Dor pulsations (Debosscher et al., 2013; Maceroni et al., 2013), δ Scuti pulsations (Southworth et al., 2011; Lehmann et al., 2013), and hybrid γ Dor- δ Scuti pulsations (Hambleton et al., 2013; Maceroni et al., 2014) in double-lined spectroscopic and eclipsing binaries followed. The studies illustrated that disentangling the pulsational variability from variability induced by the binary orbit requires careful iterative techniques (see Figure 10), and showed up limitations of current light curve modeling codes to account for complex reflection effects (e.g., Southworth et al., 2011). Each of these studies constrained the primary and secondary masses, radii and temperatures with uncertainties of a few percent, and yielded a wealth of pulsation frequencies.

Detailed asteroseismic modeling of these systems is still in progress, and first efforts have concentrated on identifying the pulsating components by modeling the expected pulsation frequency ranges of p modes and g modes based on the dynamically constrained properties. For example, Maceroni et al. (2014) showed that the estimated mean g-mode period spacing measured in the F-star eclipsing binary KIC 3858884 is only consistent with pulsations in the secondary, despite both components having similar masses and differing in radius by $\sim 10\%$. Furthermore, inclusion of convective core overshooting was required to obtain agreement with theoretical models. The exceptional amount of complementary information in KIC 3858884 and other systems promises to advance our understanding of pulsations in intermediate-mass stars in future modeling efforts.

Turning to more evolved stars, ground-based observations have yielded a handful of RR Lyrae and Cepheid pulsators in eclipsing binary systems (Pietrzyński et al., 2010; Soszyński et al., 2011). Such systems are important to test masses derived from evolutionary models, as well as to accurately measure distances through period-luminosity relations. So far, no detections of RR Lyrae or Cepheid pulsators in eclipsing binaries have been reported using space-based observations, which is likely related to the relative sparsity of such stars in the *Kepler* and CoRoT target lists.

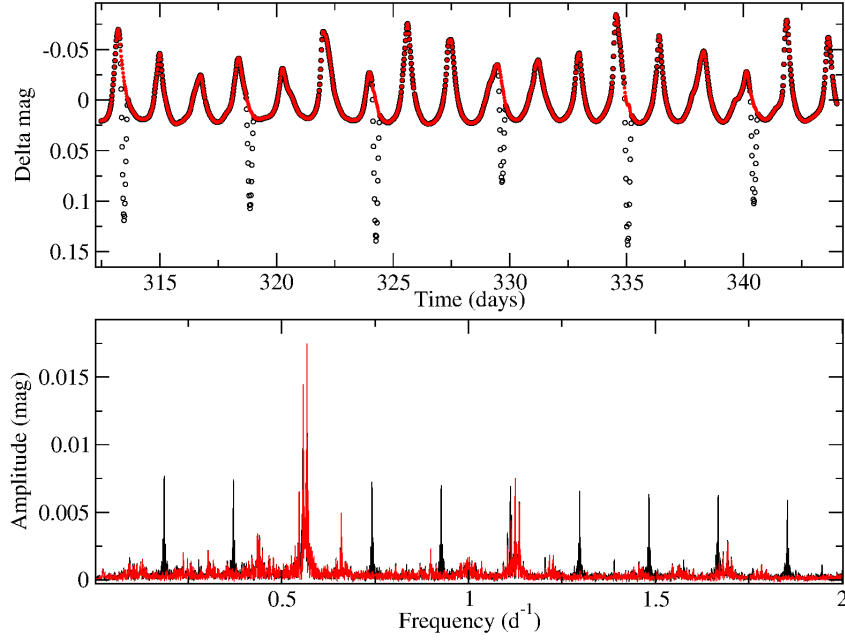


Fig. 10 Top panel: Subset of the *Kepler* light curve for KIC 11285625, a system showing eclipses with a period of 10.8 days and γ Dor pulsations with periods of $\sim 1 - 2$ days. Filled red data points show the light curve after removal of the eclipses. Bottom panel: Amplitude spectrum of the *Kepler* data before (black) and after (red) removing the eclipses. From Debosscher et al. (2013).

5.2 Compact Pulsators

Asteroseismology of white dwarfs or subdwarf B stars allows to address a wide variety of fundamental physics such as convection, crystallization, the properties of neutrinos, and the evolution on the extreme horizontal branch (see, e.g., Winget and Kepler, 2008; Heber, 2009, for reviews). Finding compact pulsators in eclipsing binary systems is extremely valuable to cross-check asteroseismically derived properties and provide independent constraints for improved seismic modeling.

Due to their faintness, the detection of pulsating white dwarfs or sdB stars in eclipsing binaries is challenging. The benchmark system is PG1336-018, a 0.1 day period eclipsing sdB - M dwarf system (Kilkenny et al., 1998). The sdB component shows p-mode pulsations with frequencies ranging from $\sim 5000 - 7000 \mu\text{Hz}$, which were subsequently combined with a full orbital solution to demonstrate that asteroseismic modeling yields a mass and radius which agrees with the dynamical estimates within 1% (Vučković et al., 2007; Van Grootel et al., 2013).

A spectacular second detection of a pulsating sdB star in an eclipsing binary has been revealed by *Kepler* (Østensen et al., 2010). KIC 9472174 (2M1938+4603,

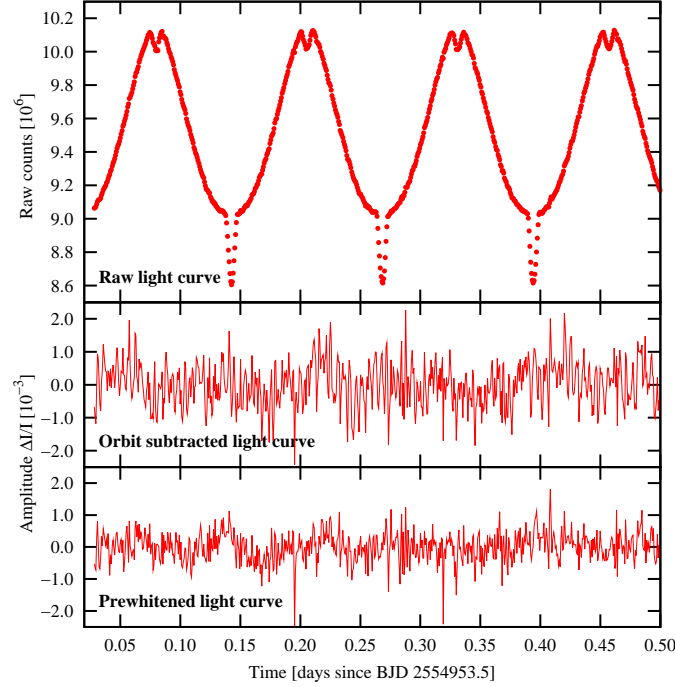


Fig. 11 Top panel: *Kepler* light curve of the eclipsing sdB+M binary KIC 9472174. Middle panel: Light curve after subtracting the orbital solution. The pulsations in the sdB star are clearly visible. Bottom panel: Residuals after subtracting the modeled pulsation frequencies. From Østensen et al. (2010).

$V \sim 12.3$) has an orbital period of 0.12 days, with strong variations due to the reflection effect in the light curve (Fig 11). After removal of a light curve model, the residuals show an unusually rich frequency spectrum in the sdB component. Østensen et al. (2010) report a total of 55 pulsation frequencies spanning from $50 - 4500 \mu\text{Hz}$, which are attributed to both p-mode and g-mode pulsations. The orbital solution combined with the radial velocity semi-amplitude and spectroscopic gravity yielded a mass of $M = 0.48 \pm 0.03 M_{\odot}$, consistent with a post common-envelope sdB star. Modeling of the pulsation frequencies is expected to yield constraints on the core structure and hence the progenitor mass of the sdB star.

Apart from KIC 9472174, *Kepler* has also uncovered several pulsating sdB stars in binaries showing light variations due to the reflection effect (Kawaler et al., 2010), which have been used to investigate tidal synchronization timescales by comparing rotation periods measured from rotational splittings to the binary period inferred from the light curve (Pablo et al., 2012). Additionally, *Kepler* has also uncovered an eclipsing (but non-pulsating) sdB + white dwarf binary which shows a combination of binary effects such as ellipsoidal deformation, Doppler beaming and microlensing (Bloemen et al., 2011).

6 Summary and Future Prospects

Table 2 summarizes the characteristics of confirmed eclipsing and/or heartbeat systems for which asteroseismic detections (either self-driven or tidally-induced) have been made using space-based observations. The list illustrates that the synergy of asteroseismology and eclipsing/eccentric binary stars using space-based observations is (unsurprisingly) still in its infancy: all of the discussed systems have been published within the last four years. Most detections were made by *Kepler*, which provided the required continuous monitoring to detect eclipses, and high-precision photometry to detect oscillations despite the dilution by the binary component or small amplitudes in the pulsating star. As noted in Section 4.1, the list of confirmed red giants in eclipsing systems can be expected to increase significantly once sufficient radial velocities have been gathered for the *Kepler* candidate systems (Gaulme et al., 2013).

Table 2 List of eclipsing and/or heartbeat systems with components showing self-excited or tidally-induced pulsations detected from space-based observations. Systems are grouped into giants (top), intermediate and high-mass stars (middle) and compact stars (bottom). Columns list the approximate *V*-band magnitude, spectral types (Sp.Type), orbital period (*P*), eccentricity (*e*), and flags indicating a double-lined spectroscopic orbit (SB2), stochastic oscillations (stoch.), self-excited coherent pulsations, tidal pulsations, eclipses (Ecl.), and heartbeat effects (HB).

ID	<i>V</i>	Sp.Type	<i>P</i> (d)	<i>e</i>	SB2	stoch.	coherent	tidal	Ecl.	HB	Ref
HD 181068	8.0	KIII+MV+MV	45.5+0.91	0.0	no	no	no	yes	yes	no	a
KIC 5006817	10.9	KIII+MV	94.8	0.71	no	yes	no	no	no	yes	b
KIC 8410637	11.3	KIII+FV	408.3	0.69	yes	yes	no	no	yes	no	c
KIC 10661783	9.5	GIV+AV	1.2	0.0	yes	no	yes	no	yes	no	d
KIC 4544587	10.8	FV+FV	2.2	0.29	yes	no	yes	yes	yes	yes	e
HD 174884	8.4	BV+Bv	3.7	0.29	yes	no	maybe	maybe	yes	yes	f
CID 102918586	11.7	FV+FV	4.4	0.25	yes	no	yes	yes	yes	yes	g
KIC 11285625	10.1	FV+FV	10.8	0.0	yes	no	yes	no	yes	no	h
KIC 3858884	9.3	FV+FV	26.0	0.47	yes	no	yes	maybe	yes	no	i
HD 187091	8.4	AV+AV	41.8	0.83	yes	no	no	yes	no	yes	j
KIC 9472174	12.3	sdB+MV	0.13	–	no	no	yes	no	yes	no	k

References: (a) Derekas et al. (2011); Borkovits et al. (2013); Fuller et al. (2013), (b) Beck et al. (2013), (c) Hekker et al. (2010); Frandsen et al. (2013), (d) Southworth (2011); Lehmann et al. (2013), (e) Hambleton et al. (2013), (f) Maceroni et al. (2009), (g) Maceroni et al. (2013), (h) Debosscher et al. (2013), (i) Maceroni et al. (2014), (j) Welsh et al. (2011), (k) Østensen et al. (2010).

Continued observations and the search for new asteroseismic eclipsing binaries remains crucial to answer important questions regarding stellar pulsations and evolution across the HRD. To highlight one particular aspect, Figure 12 shows updated empirical tests of the v_{\max} and Δv scaling relations for stochastic oscillators. Note that most points in the v_{\max} comparison are not fully independent from asteroseismology, with properties determined either by combining interferometric angular diameters with asteroseismic densities calculated from the Δv scaling

relation (e.g., Huber et al., 2012), or masses and radii determined from individual frequency modeling (e.g., Metcalfe et al., 2014). KIC 8410637 marks the first datapoint from an eclipsing binary, allowing an independent test of v_{\max} and Δv that is otherwise only possible for wide binaries with radii and masses measured from astrometry and interferometry. The Δv comparison includes four stars which host exoplanets with independently constrained eccentricities, which allows an independent measurement of the mean stellar density (Seager and Mallén-Ornelas, 2003; Winn, 2010): HD17156 (Nutzman et al., 2011; Gilliland et al., 2011), TrES-2 (Barclay et al., 2012; Southworth, 2011), Hat-P7 (Christensen-Dalsgaard et al., 2010; Southworth, 2011), and Kepler-14 (Huber et al., 2013; Southworth, 2012). Note that only stars with calculated v_{\max} and Δv with uncertainties better than 20% and 10% have been included in the comparison.

The median residuals for both quantities are close to zero, with a scatter of 7% for v_{\max} and 3% for Δv . While these numbers are encouraging, it is important to note that the observational uncertainties for v_{\max} and Δv derived from *Kepler* data are typically up to a factor of 2 or more smaller (Chaplin et al., 2014). Additionally, comparisons for evolved giant stars are essentially limited to one datapoint, yet the vast majority of stars with asteroseismic detections are giants (see Figure 3). Indeed, KIC 8410637 indicates that the v_{\max} scaling relation remains accurate for giant stars, while the Δv scaling relation predicts a density which is too low by $\sim 7\%$. Observations of stochastic oscillations in additional eclipsing binary systems will be required to investigate whether this offset may be systematic, and allow an *empirical* calibration of scaling relations.

Future observations of asteroseismic eclipsing binaries with giant and dwarf components can be expected from space-based missions such as K2 (Howell et al., 2014), TESS (Ricker et al., 2009) and PLATO (Rauer et al., 2013). Importantly, these mission will observe stars which are significantly brighter than typical CoRoT and *Kepler* targets, hence increasing the potential for independent constraints from ground-based observations such as long-baseline interferometry. There is little doubt that future space-based observations of asteroseismic eclipsing binary stars, combined with improved modeling efforts, will continue to play an important role to advance our understanding of stellar evolution across the H-R diagram.

Acknowledgements: I thank the organizers Elizabeth Griffin and Bob Stencel for a fantastic conference, and I am grateful to Paul Beck, Jørgen Christensen-Dalsgaard, Orlagh Creevey, Jonas Debosscher, Aliz Derekas, Saskia Hekker, Søren Frandsen, Jim Fuller and Roy Østensen for providing figures and comments on the manuscript. Financial support was provided by an appointment to the NASA Postdoctoral Program at Ames Research Center administered by Oak Ridge Associated Universities, and NASA Grant NNX14AB92G issued through the Kepler Participating Scientist Program.

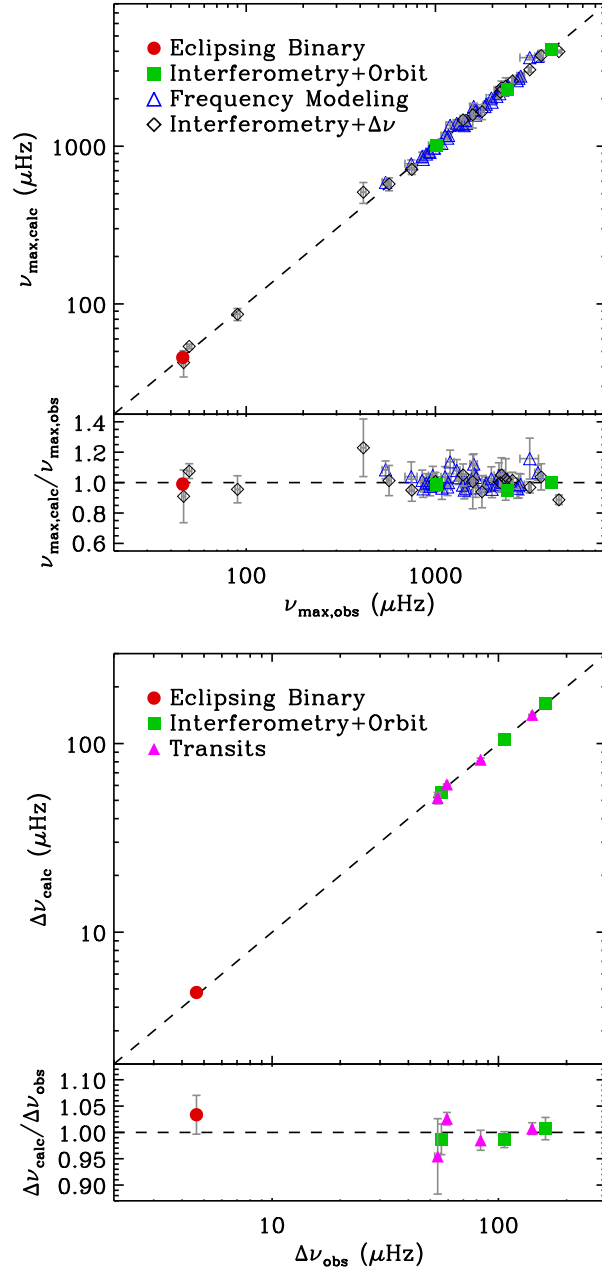


Fig. 12 Empirical tests of asteroseismic scaling relations. Top: Comparison of measured ν_{\max} values to empirical values calculated from independent measurements (see legend). Filled symbols are empirical values which are independent of asteroseismology. Bottom: Same as top figure but for the $\Delta\nu$ scaling relation.

References

- Aerts, C., 2013, in EAS Publications Series, volume 64 of EAS Publications Series, pp. 323–330
- Aerts, C., Christensen-Dalsgaard, J., and Kurtz, D.W., 2010, *Asteroseismology*, Springer: Dordrecht
- Antoci, V., Handler, G., Campante, T.L., et al., 2011, *Nature*, 477, 570
- Barclay, T., Huber, D., Rowe, J.F., et al., 2012, *ApJ*, 761, 53
- Beck, P.G., Bedding, T.R., Mosser, B., et al., 2011, *Science*, 332, 205
- Beck, P.G., Hambleton, K., Vos, J., et al., 2013, *A&A*, in press (arXiv:1312.4500)
- Bedding, T.R., 2011, ArXiv e-prints (arXiv:1107.1723)
- Bedding, T.R., Kjeldsen, H., Campante, T.L., et al., 2010, *ApJ*, 713, 935
- Bedding, T.R., Mosser, B., Huber, D., et al., 2011, *Nature*, 471, 608
- Belkacem, K., 2012, in S. Boissier, P. de Laverny, N. Nardetto, R. Samadi, D. Valls-Gabaud, and H. Wozniak, editors, SF2A-2012: Proceedings of the Annual meeting of the French Society of Astronomy and Astrophysics, pp. 173–188
- Belkacem, K., Goupil, M.J., Dupret, M.A., et al., 2011, *A&A*, 530, A142
- Bloemen, S., Marsh, T.R., Østensen, R.H., et al., 2011, *MNRAS*, 410, 1787
- Borkovits, T., Derekas, A., Kiss, L.L., et al., 2013, *MNRAS*, 428, 1656
- Bouchy, F. and Carrier, F., 2001, *A&A*, 374, L5
- Breger, M., 2000, in M. Breger & M. Montgomery, editor, *Delta Scuti and Related Stars*, volume 210 of *Astronomical Society of the Pacific Conference Series*, p. 3
- Breger, M., Balona, L., Lenz, P., et al., 2011, *MNRAS*, 414, 1721
- Brogaard, K., VandenBerg, D.A., Bruntt, H., et al., 2012, *A&A*, 543, A106
- Brown, T.M., Gilliland, R.L., Noyes, R.W., et al., 1991, *ApJ*, 368, 599
- Brown, T.M., Latham, D.W., Everett, M.E., et al., 2011, *AJ*, 142, 112
- Burkart, J., Quataert, E., Arras, P., et al., 2012, *MNRAS*, 421, 983
- Carrier, F., Bouchy, F., Kienzie, F., et al., 2001, *A&A*, 378, 142
- Carter, J.A., Agol, E., Chaplin, W.J., et al., 2012, *Science*, 337, 556
- Casagrande, L., Silva Aguirre, V., Stello, D., et al., 2014, ArXiv e-prints (arXiv:1403.2754)
- Chaplin, W.J., Basu, S., Huber, D., et al., 2014, *ApJS*, 210, 1
- Chaplin, W.J., Bedding, T.R., Bonanno, A., et al., 2011a, *ApJ*, 732, L5
- Chaplin, W.J., Kjeldsen, H., Christensen-Dalsgaard, J., et al., 2011b, *Science*, 332, 213
- Chaplin, W.J. and Miglio, A., 2013, *ARA&A*, 51, 353
- Christensen-Dalsgaard, 2003, *Lecture Notes*, Aarhus University
- Christensen-Dalsgaard, J., Kjeldsen, H., Brown, T.M., et al., 2010, *ApJ*, 713, L164
- Christiansen, J.L., Derekas, A., Ashley, M.C.B., et al., 2007, *MNRAS*, 382, 239
- Creevey, O.L., Metcalfe, T.S., Brown, T.M., et al., 2011, *ApJ*, 733, 38
- Damiani, C., Maceroni, C., Cardini, D., et al., 2010, *Ap&SS*, 328, 91
- De Ridder, J., Barban, C., Baudin, F., et al., 2009, *Nature*, 459, 398
- Debosscher, J., Aerts, C., Tkachenko, A., et al., 2013, *A&A*, 556, A56
- Derekas, A., Kiss, L.L., Borkovits, T., et al., 2011, *Science*, 332, 216
- Dziembowski, W.A., Gough, D.O., Houdek, G., et al., 2001, *MNRAS*, 328, 601

- Fabrycky, D.C., Ford, E.B., Steffen, J.H., et al., 2012, *ApJ*, 750, 114
- Frandsen, S., Lehmann, H., Hekker, S., et al., 2013, *A&A*, 556, A138
- Fuller, J., Derekas, A., Borkovits, T., et al., 2013, *MNRAS*, 429, 2425
- Fuller, J. and Lai, D., 2012, *MNRAS*, 420, 3126
- Gaulme, P., Jackiewicz, J., Appourchaux, T., et al., 2014, *ApJ*, 785, 5
- Gaulme, P., McKeever, J., Rawls, M.L., et al., 2013, *ApJ*, 767, 82
- Gilliland, R.L., Brown, T.M., Christensen-Dalsgaard, J., et al., 2010, *PASP*, 122, 131
- Gilliland, R.L., McCullough, P.R., Nelan, E.P., et al., 2011, *ApJ*, 726, 2
- Gizon, L. and Solanki, S.K., 2003, *ApJ*, 589, 1009
- Gough, D.O., 1986, in Y. Osaki, editor, *Hydrodynamic and Magnetodynamic Problems in the Sun and Stars*, p. 117, Uni. of Tokyo Press
- Grigahcène, A., Antoci, V., Balona, L., et al., 2010, *ApJ*, 713, L192
- Guenther, D.B., Kallinger, T., Reegen, P., et al., 2007, *Communications in Asteroseismology*, 151, 5
- Guzik, J.A., Kaye, A.B., Bradley, P.A., et al., 2000, *ApJ*, 542, L57
- Hambleton, K.M., Kurtz, D.W., Prša, A., et al., 2013, *MNRAS*, 434, 925
- Handler, G., 2013, *Asteroseismology*, p. 207
- Heber, U., 2009, *ARA&A*, 47, 211
- Hekker, S., Debosscher, J., Huber, D., et al., 2010, *ApJ*, 713, L187
- Hekker, S., Elsworth, Y., Basu, S., et al., 2013, *MNRAS*, 434, 1668
- Hekker, S., Elsworth, Y., Mosser, B., et al., 2012, *A&A*, 544, A90
- Hekker, S., Kallinger, T., Baudin, F., et al., 2009, *A&A*, 506, 465
- Houdek, G., Balmforth, N.J., Christensen-Dalsgaard, J., et al., 1999, *A&A*, 351, 582
- Howell, S.B., Sobeck, C., Haas, M., et al., 2014, *PASP*, in press (arXiv:1402.5163)
- Huber, D., Bedding, T.R., Stello, D., et al., 2011, *ApJ*, 743, 143
- Huber, D., Chaplin, W.J., Christensen-Dalsgaard, J., et al., 2013, *ApJ*, 767, 127
- Huber, D., Ireland, M.J., Bedding, T.R., et al., 2012, *ApJ*, 760, 32
- Huber, D., Silva Aguirre, V., Matthews, J.M., et al., 2014, *ApJS*, 211, 2
- Huber, D., Stello, D., Bedding, T.R., et al., 2009, *Communications in Asteroseismology*, 160, 74
- Kawaler, S.D., Reed, M.D., Østensen, R.H., et al., 2010, *MNRAS*, 409, 1509
- Kilkenny, D., O'Donoghue, D., Koen, C., et al., 1998, *MNRAS*, 296, 329
- Kippenhahn, R. and Weigert, A., 1994, *Stellar Structure and Evolution*, Springer: Berlin
- Kjeldsen, H. and Bedding, T.R., 1995, *A&A*, 293, 87
- Kjeldsen, H., Bedding, T.R., Butler, R.P., et al., 2005, *ApJ*, 635, 1281
- Kurtz, D.W., 1982, *MNRAS*, 200, 807
- Lai, D., 1997, *ApJ*, 490, 847
- Lehmann, H., Southworth, J., Tkachenko, A., et al., 2013, *A&A*, 557, A79
- Lehmann, H., Tkachenko, A., Semaan, T., et al., 2011, *A&A*, 526, A124
- Maceroni, C., Lehmann, H., da Silva, R., et al., 2014, *ArXiv e-prints*
- Maceroni, C., Montalbán, J., Gandolfi, D., et al., 2013, *A&A*, 552, A60
- Maceroni, C., Montalbán, J., Michel, E., et al., 2009, *A&A*, 508, 1375
- Matijević, G., Prša, A., Orosz, J.A., et al., 2012, *AJ*, 143, 123

- Matthews, J.M., 2007, *Communications in Asteroseismology*, 150, 333
- Mészáros, S., Holtzman, J., García Pérez, A.E., et al., 2013, *AJ*, 146, 133
- Metcalfe, T.S., Chaplin, W.J., Appourchaux, T., et al., 2012, *ApJ*, 748, L10
- Metcalfe, T.S., Creevey, O.L., Dogan, G., et al., 2014, *ArXiv e-prints* (arXiv:1402.3614)
- Michel, E. and Baglin, A., 2012, *ArXiv e-prints* (arXiv:1202.1422)
- Michel, E., Samadi, R., Baudin, F., et al., 2009, *A&A*, 495, 979
- Miglio, A., 2012, in A. Miglio, J. Montalbán, and A. Noels, editors, *Red Giants as Probes of the Structure and Evolution of the Milky Way*, *ApSS Proceedings*, Berlin: Springer
- Miglio, A., Brogaard, K., Stello, D., et al., 2012, *MNRAS*, 419, 2077
- Miglio, A., Chiappini, C., Morel, T., et al., 2013, in *European Physical Journal Web of Conferences*, volume 43 of *European Physical Journal Web of Conferences*, pp. 3004, DOI: 10.1051/epjconf/20134303004
- Mkrtychian, D.E., Kusakin, A.V., Rodriguez, E., et al., 2004, *A&A*, 419, 1015
- Mosser, B., Belkacem, K., Goupil, M.J., et al., 2010, *A&A*, 517, A22
- Mosser, B., Michel, E., Belkacem, K., et al., 2013, *A&A*, 550, A126
- Nemec, J.M., Cohen, J.G., Ripepi, V., et al., 2013, *ApJ*, 773, 181
- Nutzman, P., Gilliland, R.L., McCullough, P.R., et al., 2011, *ApJ*, 726, 3
- Østensen, R.H., Bloemen, S., Vučković, M., et al., 2011, *ApJ*, 736, L39
- Østensen, R.H., Green, E.M., Bloemen, S., et al., 2010, *MNRAS*, 408, L51
- Pablo, H., Kawaler, S.D., Reed, M.D., et al., 2012, *MNRAS*, 422, 1343
- Pamyatnykh, A.A., 2000, in M. Breger & M. Montgomery, editor, *Delta Scuti and Related Stars*, volume 210 of *Astronomical Society of the Pacific Conference Series*, p. 215
- Pietrinferni, A., Cassisi, S., Salaris, M., et al., 2004, *ApJ*, 612, 168
- Pietrzyński, G., Thompson, I.B., Gieren, W., et al., 2010, *Nature*, 468, 542
- Prša, A., Batalha, N., Slawson, R.W., et al., 2011, *AJ*, 141, 83
- Rauer, H., Catala, C., Aerts, C., et al., 2013, *ArXiv e-prints* (arXiv:1310.0696)
- Ricker, G.R., Latham, D.W., Vanderspek, R.K., et al., 2009, in *American Astronomical Society Meeting Abstracts 213*, volume 41 of *Bulletin of the American Astronomical Society*, p. 403.01
- Rodríguez, E. and Breger, M., 2001, *A&A*, 366, 178
- Salaris, M., Cassisi, S., Pietrinferni, A., et al., 2010, *ApJ*, 716, 1241
- Seager, S. and Mallén-Ornelas, G., 2003, *ApJ*, 585, 1038
- Silva Aguirre, V., Casagrande, L., Basu, S., et al., 2012, *ApJ*, 757, 99
- Slawson, R.W., Prša, A., Welsh, W.F., et al., 2011, *AJ*, 142, 160
- Sokolovsky, K., Maceroni, C., Hareter, M., et al., 2010, *Communications in Asteroseismology*, 161, 55
- Soszyński, I., Dziembowski, W.A., Udalski, A., et al., 2011, *Acta Astron.*, 61, 1
- Southworth, J., 2011, *MNRAS*, 417, 2166
- Southworth, J., 2012, *MNRAS*, 426, 1291
- Southworth, J., Zima, W., Aerts, C., et al., 2011, *MNRAS*, 414, 2413
- Stello, D., Bruntt, H., Preston, H., et al., 2008, *ApJ*, 674, L53
- Stello, D., Chaplin, W.J., Bruntt, H., et al., 2009, *ApJ*, 700, 1589

- Stello, D., Huber, D., Bedding, T.R., et al., 2013, *ApJ*, 765, L41
Tassoul, M., 1980, *ApJS*, 43, 469
Thompson, S.E., Everett, M., Mullally, F., et al., 2012, *ApJ*, 753, 86
Ulrich, R.K., 1986, *ApJ*, 306, L37
Van Grootel, V., Charpinet, S., Brassard, P., et al., 2013, *A&A*, 553, A97
Vandakurov, Y.V., 1968, *Soviet Ast.*, 11, 630
Vučković, M., Aerts, C., Østensen, R., et al., 2007, *A&A*, 471, 605
Welsh, W.F., Orosz, J.A., Aerts, C., et al., 2011, *ApJS*, 197, 4
White, T.R., Bedding, T.R., Stello, D., et al., 2011, *ApJ*, 743, 161
Winget, D.E. and Kepler, S.O., 2008, *ARA&A*, 46, 157
Winn, J.N., 2010, *ArXiv e-prints* (arXiv:1001.2010)
Winn, J.N., Fabrycky, D., Albrecht, S., et al., 2010, *ApJ*, 718, L145
Zahn, J.P., 1975, *A&A*, 41, 329